

# Analysis of RF-MEMS Switches Using Finite Element-Boundary Integration with Moment Method

Zhongde Wang\*, Brian Jensen, John Volakis, Kazuhiro Saitou, Katsuo Kurabayashi

University of Michigan, Ann Arbor

**Abstract**—This paper presents a new hybrid methodology for modeling RF-MEMS switches. This method combines the usual finite element-boundary integration (FE-BI) method for the fixed section of the switch, and the method of moment for the movable beam. This approach is intended to address the large 100:1 scale variation within a single computational domain, which also spans a very small fraction of a wavelength.

**Index Terms**—Finite element method (FEM), boundary integration (BI), method of moment (MOM), radio-frequency microelectromechanical systems (RF-MEMS)

## I. INTRODUCTION

RF MEMS switches have demonstrated low on-state insertion loss, high off-state isolation, and very linear behavior [1-6]. Despite these excellent characteristics, they generally suffer from low power-handling capability, with most switches operating well below 1 W [4]. This limitation is due to the complex interactions among electromagnetic losses, heat transfer, and mechanical deformations within and surrounding MEMS switches. In order to overcome this limitation, therefore, an accurate multiphysics modeling capturing the coupling among electromagnetic, thermal and mechanical domains is desired [7]. As a first attempt towards this end, this paper presents the development of an electromagnetic model that allows accurate material and surface modeling of intricate details within a small volume enclosing a MEMS switch.

Fig.1 illustrates a typical RF-MEMS contact switch referred in the model development below. It consists of a fixed-fixed micromachined beam of 100 to 600  $\mu\text{m}$  long, suspended above the substrate by a gap of 1 - 3  $\mu\text{m}$ . At 2 GHz, for example, these dimensions correspond to an electrical length of  $\lambda/1500$  to  $\lambda/250$  and a gap of  $\lambda/150,000$  to  $\lambda/50,000$ . The total size of the MEMS device is thus many times smaller than the typical element sizes in an FEM or FDTD code (approximately  $\lambda/20$  to  $\lambda/10$ ) [8,9]. Therefore, modeling a switch and its surrounding environment with these methods would require a large number of unknowns and a large computational time. Computer codes which assume a larger element size may also use simplifying assumptions which do not apply well to such electrically small parts. Moreover, the beam moves up and down to switch on and off. Therefore, any modeling scheme that meshes the volume under the beam, such as the FEM or FDTD, requires remeshing of the system for up- and down-states. Because a regular rectangular mesh is often used, FDTD is also poorly-suited to model the deflected beam in the down state, when the beam is no longer flat.

For these reasons, the method of moments (MOM) is preferred. However, if the switch is part of a more complicated system, such as a multi-layer reconfigurable antenna including FSS elements, finite element methods may be preferred to model the complex geometry and different materials in the system. This motivated the development of a combined FE-BI and MOM presented in this paper. In contrast to conventional hybrid FE-BI methods [10], the present development allows for boundary integrals which are not enclosing an FEM domain, realizing a greater flexibility to model deformed 3D surfaces in RF-MEMS switches without introducing significant computational expense.

## II. MODEL FORMULATION

In our new model, FE-BI is used for the fixed portion of the switch ( $S_1$  in Fig.1) whereas MOM is used for the MEMS beam ( $S_2$  in Fig.1). A special challenge is to formulate the connectivity of non-

---

This work is supported by the National Science Foundation under grant no. ECS-01152222

conformal BI with the BI bounding the FEM region. Assuming some excitation currents  $(\vec{J}, \vec{M})$ , the usual weak form of the FE-BI [8] for the fixed portion of the switch  $S_f$  is given as

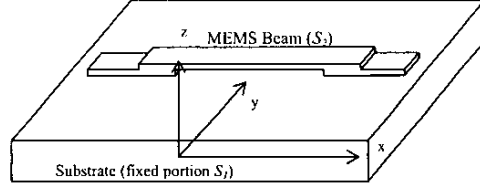


Fig.1 A typical RF-MEMS Switch

$$\iiint_V \left\{ \left( \frac{1}{\mu_r} \nabla \times \vec{E} \right) \cdot (\nabla \times \vec{T}) - k_0^2 \epsilon_r \vec{E} \cdot \vec{T} \right\} dv \quad (1)$$

$$+ jk_0 Z_0 \oint_{S_f} (\vec{H}^{S_1} + \vec{H}^{S_2}) \times \hat{n} \cdot \vec{T} ds = - \iiint_V \left\{ jk_0 Z_0 \vec{J}' + \nabla \times \left( \frac{1}{\mu_r} \vec{M}' \right) \right\} \cdot \vec{T} dv$$

$$\vec{H}^{S_1} = j \frac{2k_0}{Z_0} \iint_{S_1} \vec{\bar{G}}_0(\vec{r}, \vec{r}') \cdot \vec{M}'(\vec{r}') ds' \quad (1a)$$

$$\vec{H}^{S_2} = - \iint_{S_2} \nabla \times \vec{\bar{G}}_1(\vec{r}, \vec{r}') \cdot \vec{J}_{S_2}(\vec{r}') ds' \quad (1b)$$

where

- $\vec{M}'_{S_1}$ : the currents/fields enclosing the fix portion region ( $S_1$  see Fig. 1);
- $\vec{J}'_{S_2}$ : the current on the MEMS beam external to the FE-BI region ( $S_2$  see Fig. 1);
- $\vec{r}'_i$ : image point of source point  $\vec{r}'$ ;  $k_0$ : wavelength number;  $Z_0$ : free-space impedance;
- $\vec{M}'(\vec{r}) = \vec{E}'(\vec{r}) \times \hat{n}$ : equivalent magnetic current;
- $\vec{J}'(\vec{r}) = \hat{n} \times \vec{H}'(\vec{r})$ : equivalent electric current;
- $\vec{\bar{G}}_0(\vec{r}, \vec{r}') = \left( \vec{I} + \frac{1}{k_0^2} \nabla \nabla \right) G_0(\vec{r}, \vec{r}')$ : free-space Dyadic Green Function;
- $\vec{\bar{G}}_1(\vec{r}, \vec{r}') = \left( \vec{I} - \frac{1}{k_0^2} \nabla \nabla \right) \left( G_0(\vec{r}, \vec{r}') - G_0(\vec{r}, \vec{r}'_i) \right) + 2\hat{z}\hat{z}G_0(\vec{r}, \vec{r}'_i)$ : half-space Dyadic Green Function;

In order to solve equation (1) for  $\vec{M}'_{S_1}$  and  $\vec{J}'_{S_2}$ , the additional set of equations is required to enforce boundary conditions on the MEMS beam  $S_2$ . Using MOM, this can be given as:

$$\hat{n} \times \left[ \vec{E}^{S_1}(\vec{M}) + \vec{E}^{S_2}(\vec{J}_{S_2}) \right] = 0 \quad (2)$$

$$\vec{E}^{S_1} = - \iint_{S_1} \nabla \times \vec{\bar{G}}_0(\vec{r}, \vec{r}') \cdot \vec{M}'(\vec{r}') ds' \quad (2a)$$

$$\vec{E}^{S_2} = -jk_0 Z_0 \iint_{S_2} \vec{\bar{G}}_1(\vec{r}, \vec{r}') \cdot \vec{J}_{S_2}(\vec{r}') ds' \quad (2b)$$

Here, brick elements are used for the substrate to reduce the number of unknowns, and triangular surface elements are applied on the MEMS beam for more flexible modeling of a deformed beam surface. Using Galerkin's method yields the following matrix system [8]:

$$\begin{bmatrix} A^{I'V} & A^{VS_1} & 0 \\ A^{S_1I'} & A^{S_1S_1} & A^{S_1S_2} \\ 0 & A^{S_2S_1} & A^{S_2S_2} \end{bmatrix} \begin{Bmatrix} E_n^{I'} \\ E_n^{S_1} \\ J_n^{S_2} \end{Bmatrix} = \begin{Bmatrix} b_m^{I'} \\ b_m^{S_1} \\ 0 \end{Bmatrix} \quad (3)$$

where  $[A^{I'V}]$ ,  $[A^{VS_1}]$ ,  $[A^{S_1I'}]$  and  $[A^{S_1S_1}]$  represent the FE-BI system (1) for the fixed volume enclosed by  $S_1$ . As usual,  $[A^{I'V}]$ ,  $[A^{VS_1}]$ ,  $[A^{S_1I'}]$  are very sparse but  $[A^{S_1S_1}]$  is dense. Similarly,  $[A^{S_2S_1}]$  and  $[A^{S_2S_2}]$  are the matrices representing the interaction between the beam and the BI enclosing substrate. They are dense, as is  $[A^{S_2S_2}]$ , a submatrix representing the discretized MOM system (2).

### III. NUMERICAL EXAMPLES

A FORTRAN program was developed to calculate the current density along the beam and field patterns inside the underlying substrate. In developing this code, special care was required to evaluate all singular portions of the boundary integrals and their interactions [12]. Our code is capable of handling beams with more realistic dimensions (~100  $\mu\text{m}$ ); however, in order to be compared with available codes, in the following examples we assume a substrate with height=0.25cm, width=2cm, length=4cm, and  $\epsilon_r = 4$ . The working frequency is 3GHz and a current dipole source was put at the center of the top surface of the substrate carrying one ampere ( $0^\circ$  phase).

First we considered a plane beam (up-state of the RF-MEMS switch) with length=1.5 cm, width=1cm and gap height=0.15 cm. The beam current as compared to another FE-BI code, AMPHIA [11] is shown in Fig.2. Clearly the agreement is not perfect but reasonable. The main reason for the disagreement is likely due to the ground plane under and around the substrate in this implementation, whereas AMPHIA does not consider this ground plane.

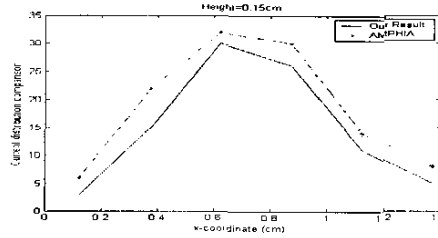


Fig.2 Current distribution along a plane (up-state) MEMS beam

To consider the down-state of the RF-MEMS switch, a piecewise 3-sectional linear approximation of the curved beam model was considered, shown in Fig. 4. The size is the same as the previous example, with the only difference being the gap of  $h_2 = 0.1\text{cm}$  from the center to the edge. Fig. 3 shows the current distribution along the beam without junctions compared to a commercial software code HFSS. Our results matches very well with HFSS when  $h_1 \geq 0.1\lambda$ , and the difference also is mainly because HFSS does not consider the infinite ground plane effect. Again, for  $h_1 \ll 0.1\lambda$  the modeling accuracy of traditional approaches is of issue.

It should be emphasized that the computational efficiency of our method over HFSS is increased dramatically due to significantly smaller numbers of unknowns (128 bricks with 48 triangles in our method versus 11946 tetrahedral elements in HFSS).

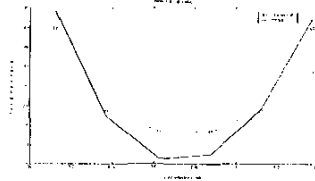


Fig.3 Current distribution along a curved beam

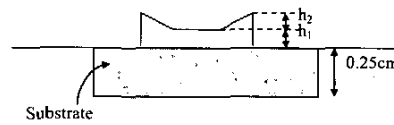


Fig.4 Piecewise linear approximation of a curved (down state) MEMS beam

#### IV. CONCLUSION

This paper has demonstrated a combined FE-BI and moment method approach for analyzing MEMS structures. This new hybrid method allows for flexible and accurate modeling of the moving and stationary portions of the RF-MEMS switches without significant computational expenses. As such, it can be effectively integrated with mechanical and thermal modeling for a true multiphysics analysis.

#### REFERENCES

- [1] Yao, J.J., "RF-MEMS from device perspective", *J. Micromech. and Microeng.*, Vol. 10 (2000), pp. R8-R38.
- [2] Pacheco, S., Nguyen, C.T., and Katchi, L.P.B., "Micromechanical Electrostatic K-Band Switches," *1998 IEEE MTT-S Digest*, 1998, pp. 1569-1572.
- [3] Zavracky, P.M., McGruer, N.E., Morrison, R.H., and Potter, D., "Microswitches and Microrelays with a View Toward Microwave Applications," *Int. J. RF and Microwave Theory and Techniques*, Vol. 9, No. 4 (1999), pp. 338-347.
- [4] Rebeiz, G.M. and Muldavin, J.B., "RF MEMS Switches and Switch Circuits," *IEEE Microwave Mag.*, Vol. 2, No. 4 (Dec. 2001), pp.59-71.
- [5] Duffy, S., Bozler, C., Rabe, S., Knecht, J., Travis, L., Wyatt, P., Keast, C., and Gouker, M., "MEMS Microswitches for Reconfigurable Microwave Circuitry," *IEEE Microwave and Wireless Components Letters*, Vol. 11, No. 3 (Mar. 2001), pp. 106-108.
- [6] Muldavin, J.B. and Rebeiz, G.M., "Inline Capacitive and DC-Contact MEMS Shunt Switches," *IEEE Microwave and Wireless Components Letters*, Vol. 11, No. 8 (Aug. 2001), pp. 334-336.
- [7] Jensen, B.D., Saitou, K., Volakis, J.L., and Kurabayashi, K., "Impact of Skin Effect on Thermal Behavior of RF MEMS Switches," *6th ASME-JSME Thermal Engineering Joint Conference*, Paper No. TED-AJ03-420, March 2003.
- [8] Volakis, J.L., Chatterjee, A., and Kempel, L.C., *Finite Element Method of Electromagnetics*, New York, IEEE Press, 1998.
- [9] Taflov, A., Hagness, S.C., *Computational Electrodynamics: The Finite-Difference Time-Domain Method*, Artech House, 2000.
- [10] Jin, J.M., Volakis, J.L., and Collins, J.D., "A finite element-boundary integral method for scattering and radiation by two- and three-dimensional structures," *IEEE Antennas Propagat. Soc. Mag.*, Vol. 33, No. 3 (June 1991), pp. 22-32.
- [11] R. Kindt, K. Sertel, E. Topsakal, and J. L. Volakis, "Array Decomposition Method for the Accurate Analysis of Finite Arrays," *to appear in IEEE Trans. Antennas Propagat.*, May 2003
- [12] R. D. Graglia, "On the numerical integration of linear shape functions times the 3-D Green's function or its gradient on a plane triangle," *IEEE Trans. Antenna Propagation*, vol. 41, no. 10, pp. 1448-1455, Oct. 1993